Genetically encoded reporters of protein kinase A activity reveal impact of substrate tethering

Jin Zhang*, Yuliang Ma†‡, Susan S. Taylor†‡, and Roger Y. Tsien*†‡§

Departments of *Pharmacology and †Chemistry and Biochemistry, and ‡Howard Hughes Medical Institute, University of California at San Diego, 9500 Gilman Drive, La Jolla, CA 92093

Contributed by Susan S. Taylor, October 23, 2001

The complexity and specificity of many forms of signal transduction are widely suspected to require spatial microcompartmentation of protein kinase and phosphatase activities, yet current relevant imaging methods such as phosphorylation-specific antibodies or fluorescent peptide substrates require fixation or microinjection and lack temporal or spatial resolution. We present a genetically encoded fluorescent reporter for protein kinase A (PKA) consisting of fusions of cyan fluorescent protein, a phosphoamino acid binding domain (14–3-3τ), a consensus substrate for PKA, and yellow fluorescent protein. cAMP elevations cause 25–50% changes in the ratios of yellow to cyan emissions in live cells caused by phosphorylation-induced changes in fluorescence resonance energy transfer. The reporter response was accelerated by tethering to PKA holoenzyme and slowed by localization to the nucleus. We demonstrate that deliberate redistribution of a substrate or colocalizing a substrate and PKA can modulate its susceptibility to phosphorylation by the kinase. The successful design of a fluorescent reporter of PKA activity and its application for studying compartmentalized and dynamic modulation of kinases lays a foundation for studying targeting and compartmentation of PKA and other kinases and phosphatases.

Protein phosphorylation/dephosphorylation is the most important way that cellular proteins are posttranslationally modified to modulate their function. In many cases, spatial microcompartmentation of protein kinase and phosphatase activities is required to achieve specific and optimized modulation in signaling events. In the case of cAMP-dependent protein kinase A (PKA), given its ubiquitous presence in mammalian cells and its widespread involvement in numerous parallel signaling cascades, understanding the functional complexities of how the kinase is activated in the right place at the right time inside cells is important. This specificity is achieved, in part, through the compartmentation of PKA at discrete subcellular locations through interaction with a family of specific anchor proteins (A-kinase anchor proteins, AKAPs) (1–3). Localization recruits the PKA holoenzyme close to its substrate/effector proteins, thereby directing and modulating the biological effects of cAMP signaling. Disruption of PKA anchoring by peptides that antagonize PKA–AKAP interactions often disables cAMP-dependent signaling (4, 5), emphasizing the essential role of PKA anchoring in signal transduction. Compartmentation of other kinases, phosphatases, and substrates is widely conjectured to be a key determinant in the specificity of other signaling pathways, although the molecular basis and cellular consequences of such compartmentation are less well understood (6, 7).

Direct detection of compartmentalized activities of kinases and phosphatases is a major challenge to the spatial and temporal resolution of current methods. Immunocytochemistry with phosphorylation-specific antibodies (8–10) is rarely quantitative and requires cell fixation and permeabilization; thus temporal resolution is poor. Fluorescently labeled peptide substrates for kinases (11–14) require microinjection, are subject to proteolysis, cannot easily be targeted, and therefore suffer from relatively poor spatial resolution.

Genetically encoded indicators with conformationally responsive or cleavable natural or chimeric proteins sandwiched between two mutants of green fluorescent protein (GFP) capable of fluorescence resonance energy transfer (FRET) have successfully monitored Ca^{2+} (15–17), Zn^{2+} (18), cAMP (19), and cGMP (20, 21) fluctuations, as well as protease (22–24) and Ras/Rap1 activities (25) in live cells. Previously, green and blue variants of GFP have been fused to the N and C termini of a 19-residue peptide derived from the cAMP response element binding protein (CREB). Phosphorylation by PKA modestly decreased FRET from blue fluorescent protein to the GFP (26). However, indicators based on blue fluorescent proteins are difficult to use because of the poor photostability of the latter. Furthermore, we desired a more general and robust strategy for generating larger fluorescence changes from any kinase for which the consensus phosphorylation site is known.

The most general strategy is to take advantage of the recent expansion in the knowledge of phosphoamino acid binding domains and to use the intramolecular complexation between a phosphorylated peptide and the concatenated phosphoamino acid binding domain upon phosphorylation as a reliable source of conformational change. Two GFP mutants could be joined by a tandem fusion domain composed of a substrate domain for the protein kinase, a flexible linker sequence, and a phosphorylation recognition domain that binds the phosphorylated substrate domain. The kinase of interest should phosphorylate the substrate peptide sequence, whereupon the phosphorylation recognition domain should form an intramolecular complex with the phosphorylated peptide. This conformational change alters the distance and/or relative orientation between the two GFP proteins and generates a FRET change. Dephosphorylation of the peptide by a phosphatase should reverse the FRET change. Here we present a generalizable example of a genetically encoded A-kinase activity reporter (AKAR) and its applications for elucidating the effects of substrate anchoring on phosphorylation kinetics in live cells.

Experimental Methods

Gene Construction. The cDNA of enhanced cyan fluorescent protein (ECFP) and citrine [a version of enhanced yellow fluorescent protein (YFP), ref. 17] were fused to 14–3-3τ (1–232) created by PCR using the template 14–3-3τ (27) and primers containing the gene sequence for the linkers and phosphorylation substrate regions. *Sph*I and *Sac*I sites were incorporated at the 5′ and 3′ ends of the gene, respectively (GenBank accession no. AF440230). Mutation S475A and K280E were incorporated by the QuickChange method (Stratagene). Constructs were cloned into pRSET$_B$ (Invitrogen) for bacterial expression. For mammalian ex-

Abbreviations: AKAP, A-kinase anchor protein; AKAR, A-kinase activity reporter; Bt$_2$cAMP, N^6,2′-*O*-dibutyryl cAMP; DMNB-cAMP, *P*-(4,5-dimethoxy-2-nitrobenzyl) cAMP; ECFP, enhanced cyan fluorescent protein; FRET, fluorescence resonance energy transfer; FsK, forskolin; GFP, green fluorescent protein; PKA, protein kinase A; PKC, protein kinase C; PKG, protein kinase G; YFP, yellow fluorescent protein.

Data deposition: The sequence reported in this paper has been deposited in the GenBank database (accession no. AF440230).

§To whom reprint requests should be addressed at: 310 CMM-W 0647, University of California at San Diego, 9500 Gilman Drive, La Jolla, CA 92093-0647. E-mail: rtsien@ucsd.edu.

The publication costs of this article were defrayed in part by page charge payment. This article must therefore be hereby marked "*advertisement*" in accordance with 18 U.S.C. §1734 solely to indicate this fact.

pression, the chimeric proteins were subcloned into pcDNA3 (Invitrogen) behind a Kozak sequence using the *Hin*dIII and *Eco*RI sites. The RPP8 fused construct was prepared by inserting two short fragments at the 3′ end of the AKAR1 gene: a 120-nt *Eco*RI–*Sal*I fragment encoding residues 333–372 of D-AKAP2 (28), followed by a 30-nt *Sal*I–*Xho*I fragment encoding the FLAG tag. The RIIα fused constructs were prepared by ligating the gene for mouse RIIα to the 5′ end of the AKAR1 gene, using an incorporated *Bam*HI site corresponding to a linker of Gly-Ile. For nuclear localization, the nuclear localization signal PKKKRKVEDA was added to the C terminus by subcloning.

Protein Expression, *in Vitro* Spectroscopy, and Phosphorylation Reactions. Chimeric proteins were expressed as N-terminal His_6 tag fusions in *Escherichia coli* and purified by nickel chelate chromatography as described (18).

Recombinant proteins were treated with the catalytic subunit of PKA (NEB, Beverly, MA; 2.5 units/μl), calmodulin-dependent protein kinase II (NEB; 5 units/μl), protein kinase C (PKC) βII and PKCδ (generous gifts from A. Newton, University of California, San Diego; 3 units/μl), or protein kinase G (PKG; Calbiochem, 4 units/μl) in the corresponding kinase reaction buffer at 25°C. The fluorescence spectra were measured with an excitation wavelength of 434 nm before and after adding ATP (typically 200 μM-1 mM) to the rest of the components. Incorporation of ^{32}P was measured by incubating different constructs with 7.5 units of PKA catalytic subunit and 6.5 nM (1.2 μCi) γ-^{32}P ATP (6,000 Ci/mmol, NEN) in PKA buffer in a total volume of 30 μl at 25°C for 30 min to 12 h. Reaction aliquots (10 μl) were spotted onto phosphocellulose, immersed in 0.5% H_3PO_4, and washed with the same solution three times for 10 min each before scintillation counting of ^{32}P.

For dephosphorylation assays, the prephosphorylated His_6-tagged reporters were first purified by Ni-NTA agarose to remove kinase and ATP, then protein phosphatase-1 (New England Biolabs) or protein phosphatase-2A (Upstate Biotechnology, Lake Placid, NY) was added at 25°C.

Cell Culture and Immunoblot Analysis. HeLa, Chinese hamster ovary, COS-7, and HEK293 cells were plated onto sterilized glass coverslips in 2-cm dishes or 10-cm plates and grown to 50–90% confluency in DMEM supplemented with 10% FBS at 37°C in 6% CO_2. Cells were then transfected with the FuGENE-6 transfection reagent (Roche Molecular Biochemicals). HeLa cells expressing the reporter were stimulated with 50 μM forskolin (FsK) for 30 min at 25°C. The cells were lysed with an ice-cold lysis buffer and the crude protein samples were concentrated and separated by SDS/PAGE and transferred onto nitrocellulose membrane, which was probed with antiphospho-PKA-substrate antibody (New England Biolabs).

Imaging. After 24- to 72-h incubation at 37°C in culture medium, the cells were washed twice with Hanks' balanced salt solution buffer, maintained in buffer in the dark at room temperature, with addition of FsK (Calbiochem), isoproterenol (Aldrich), and N^6,2′-*O*-dibutyryl cAMP (Bt_2cAMP) (Calbiochem) as indicated. For inhibition studies of PKA activity, 25 μM H-89 was added to the cells before FsK stimulation.

For uncaging of cAMP, cells were incubated with 2–200 μM of a membrane-permeant, photolyzable derivative, 4,5-dimethoxy-2-nitrobenzyl cAMP (DMNB-cAMP), then exposed for 5 s to $\approx$0.5 W/cm^2 of 340–370 nm illumination from the microscope's xenon lamp filtered through a 330WB80 filter. This UV exposure was calculated to uncage >90% of the DMNB-cAMP within the cell.

Cells were imaged on a Zeiss Axiovert microscope with a cooled charge-coupled device camera (Photometrics, Tucson, AZ), controlled by METAFLUOR 2.75 software (Universal Imaging, West Chester, PA). Dual-emission ratio imaging used a 440DF20 excitation filter, a 455DRLP dichroic mirror and two emission filters (480DF30 for ECFP, 535DF25 for citrine) altered by a filter changer (Lambda 10–2, Sutter Instruments, San Rafael, CA). Fluorescence images were background-corrected. Exposure time was 100–1,000 ms, and images were taken every 5–15 s. Measurements of FRET by trypsinolysis *in vitro* and by acceptor photobleaching in intact cells were performed as described (18).

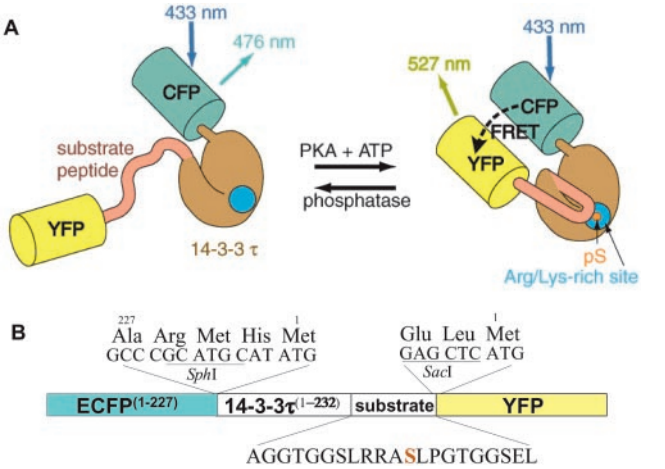

Fig. 1. Schematic representation of ratiometric indicator for visualizing protein phosphorylation (*A*) and domain structure of AKAR1 (*B*). The genes for ECFP and 14–3-3 were linked by using a *Sph*I site; the nucleotide sequences corresponding to the *Sph*I are underlined. The underlined sequences between the substrate sequence and YFP correspond to a *Sac*I site.

Results

Developing a AKAR and *in Vitro* Characterization. In our design, AKAR is a four-part chimeric protein consisting of CFP, a phosphoamino acid binding domain (14–3-3τ), a PKA-specific phosphorylatable peptide sequence, and YFP (Fig. 1*A*). 14–3-3 mediates signal transduction by binding to phosphoserine/threonine-containing proteins (29, 30). Its consensus sequence R(R/K)(F/R/S/Y)(R/H/K)pS(W/Y/F/L)P (31), where pS denotes phosphoserine, encompasses a consensus sequence for PKA phosphorylation. The C-terminal tail of 14–3-3τ was replaced by a flexible linker and another flexible linker was inserted between the substrate peptide and YFP. We chose ECFP and citrine as the FRET donor and acceptor, respectively. Citrine is currently our preferred YFP for maximum resistance to pH changes, Cl^-, photobleaching, and difficult expression conditions (17).

We generated a number of chimeras among which those containing kemptide (32) or modified kemptide as the substrate sequences were efficiently phosphorylated by the catalytic subunit of PKA (data not shown). Phosphorylation increased the citrine emission at 527 nm at the expense of the ECFP emission bands at 475–500 nm, indicating a substantial increase in FRET between the two fluorophores (Fig. 2*A*). Of all of the tested constructs, one chimera (designated as AKAR1) containing 14–3-3τ (1–232), modified kemptide (LRRASLP), and adjusted linkers (Fig. 1*B*) gave the best response to PKA, generating an emission ratio change of 30% in 5–10 min. The FRET efficiencies were quantified by using trypsin to separate the ECFP and citrine without destroying either fluorescent protein (18). Because the emissions of the ECFP in the intact chimera before and after phosphorylation were, respectively, 13% and 23% less than that after trypsinolysis of the linker (Fig. 2*A*), the corresponding FRET efficiencies were 13% and 23%. Omission of either PKA or ATP prevented the FRET change, showing that the response requires PKA phosphorylation (Fig. 2*B*).

To test whether the *in vitro* FRET change was reversible, the phosphorylated reporter was repurified and treated with phosphatases. Protein phosphatase-1 caused FRET to decrease in a time-

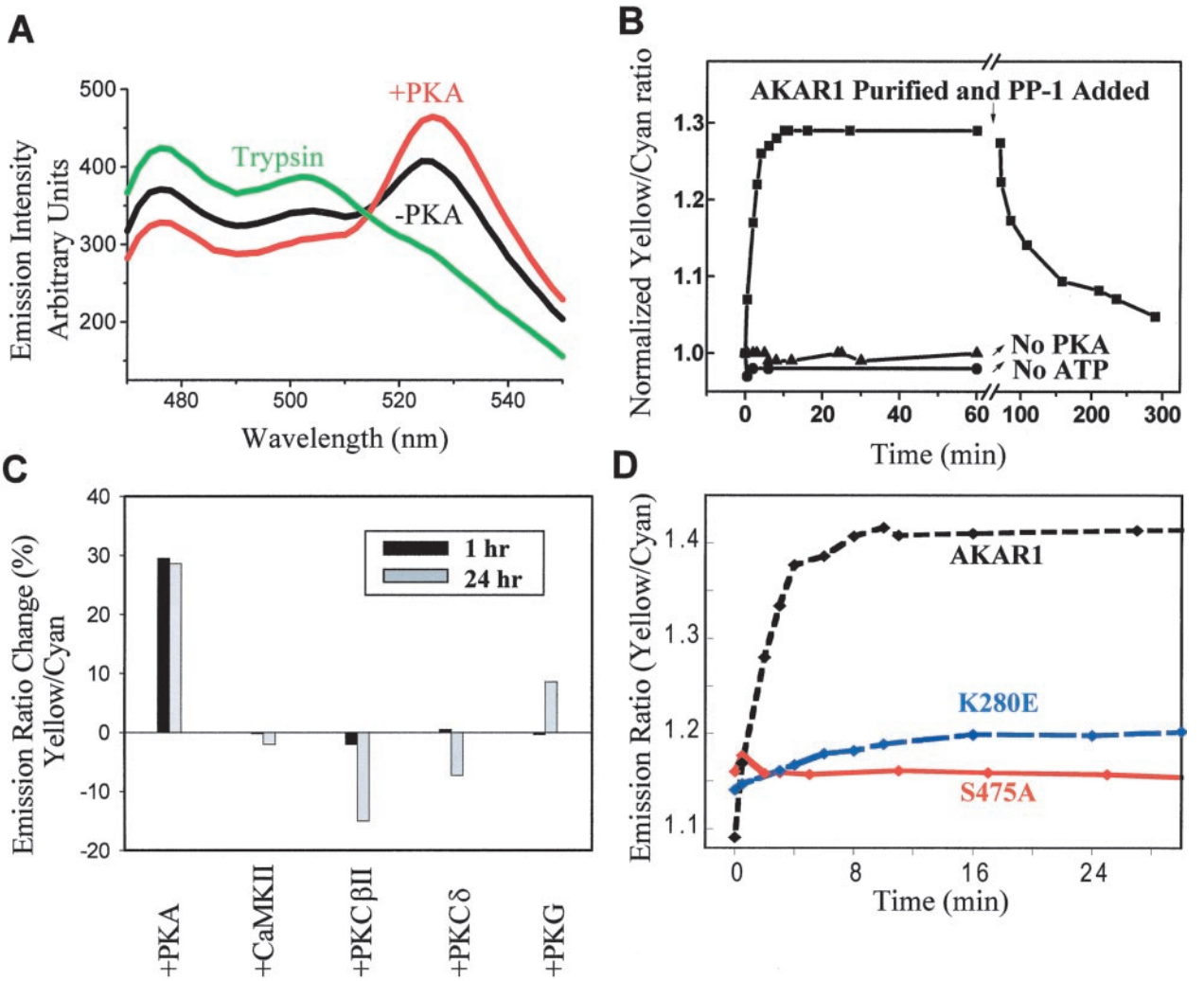

Fig. 2. *In vitro* characterization of AKAR1. (*A*) Emission spectra of the purified AKAR1 before (black) and after (red) phosphorylation by PKA (excitation 434 nm). The green curve depicts the spectrum of the reporter after digestion with trypsin to quench the energy transfer and quantify the FRET. (*B*) Phosphorylation time course for AKAR1 with the control of lacking either PKA or ATP. (*C*) Percent emission ratio change for the AKAR1 in response to *in vitro* phosphorylation by different kinases. Black and gray columns represent the percent change in 1 h and 24 h after addition of ATP, respectively. CaMKII, calmodulin-dependent protein kinase II. (*D*) Phosphorylation time course for AKAR1 and mutants S475A and K280E to validate the mechanism of intramolecular complexation.

dependent manner back to the value for unphosphorylated reporter (Fig. 2*B*). However, protein phosphatase-2A was unable to reverse the FRET increase (data not shown), so not all phosphatases are effective.

We tested the reporter *in vitro* against calmodulin-dependent protein kinase II, PKCβII, PKCτ, and PKG as representative Ser/Thr kinases whose consensus sequences have some overlap with modified kemptide. As shown in Fig. 2*C*, none of these kinases gave significant FRET changes in 1 h, but over 24 h PKC caused a small decrease in FRET whereas PKG generated a 14% emission ratio increase. Therefore AKAR1 seems completely unresponsive to calmodulin kinase II and PKCδ and only very weakly sensitive to PKCβII and PKG.

Several reporter mutants were tested to validate phosphorylation-dependent complexation of the modified kemptide by 14–3-3 as a mechanism for the FRET responses (Fig. 2*D*). Substitution of Ser to Ala (S475A) in the kemptide phosphorylation site (LRRAS^{475}LP) abolished the FRET response, demonstrating that the crucial phosphorylation is at the designed serine. The phosphoserine-binding site of 14–3-3 includes a patch of crucial basic residues. Charge-reversal mutations at these positions are known to decrease or abolish the binding of 14–3-3 to partners such as Raf-1 kinase. Mutation of one critical residue (K280E) (33) at the active site of 14–3-3 decreased the amplitude FRET response to 7–8% with little effect on kinetics. These results are consistent with the designed mechanism for FRET sensing of phosphorylation. The 14–3-3 domain from which the reporter was constructed exists naturally as a dimer (29); analytical ultracentrifugation confirmed that the reporter is likewise dimeric (data not shown), even after numerous deletions in the putative N-terminal dimerization domain of 14–3-3. Therefore it remains possible that the phosphorylated peptide binds to the 14–3-3 domain of a tightly prebound partner molecule rather than the same chimera, although the sensitivity of FRET response to the length of the linkers suggests intramolecular complexation.

Cellular Response. When AKAR1 was transfected into HeLa cells, the fluorescence was uniformly distributed in the cytosolic compartment but excluded from the nucleus (Fig. 3*A*, leftmost frame), as expected for an 82-kDa protein without targeting signals. A similar expression pattern was observed in COS-7, HEK293, and Chinese hamster ovary cells (data not shown). The remaining frames of Fig. 3*A* show pseudocolor images of yellow to cyan emission ratios before and at different times after stimulation with

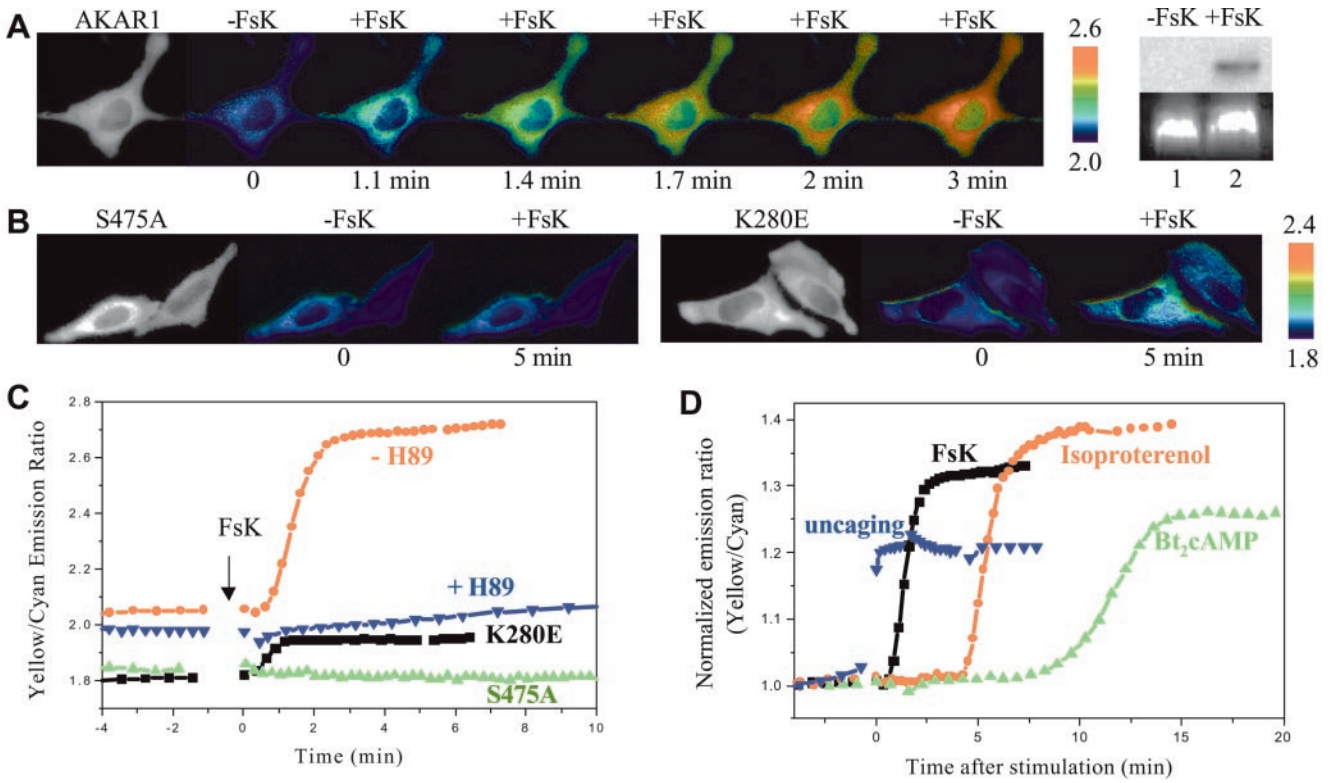

Fig. 3. Cellular responses of AKAR1. (*A*) FRET response of HeLa cells transfected (24 h) with AKAR1. (*Left*) The CFP-only image on the far left shows that the reporter distributes evenly throughout the cytosol. Pseudocolor images depict the FRET response of the reporter to FsK stimulation. (*Right*) (*Upper*) The antiphospho-PKA-substrate Western blot analysis of AKAR1 from HeLa cells; (*Lower*) the fluorescence image [470 ± 20 nm excitation, 530 ± 20 nm emission (YFP only)] of the same gel. Lane 1: AKAR1 from unstimulated cells. Lane 2: Treatment with 50 μM FsK for 30 min increases the phosphorylation level of the reporter. (*B*) FRET response of the S475A mutant (*Left*) and the K280E mutant (*Right*) of AKAR1. The height of the frames in *A* corresponds to 69 μm. Similar magnifications apply to *B*. (*C*) Emission ratio time courses for AKAR1 stimulated with 50 μM FsK in the absence and presence of the PKA inhibitor H89 (25 μM), and the S475A mutant and the K280E mutant stimulated with FsK (50 μM) in the absence of the inhibitor. (*D*) Emission ratio time courses of AKAR1 stimulated with 50 μM FsK, 1 mM Bt_2cAMP, 100 μM isoproterenol, and 50 μM of DMNB-cAMP followed by UV uncaging.

50 μM FsK to activate adenylyl cyclase and elevate cAMP. The emission ratio increase was detectable within several seconds and reached a plateau of 25–50% within 3–5 min (Fig. 3 *A* and *C*). The FRET change occurred evenly throughout the entire cytoplasm and consisted of reciprocal increases in yellow and decreases in cyan emission. Intracellular FRET efficiencies were measured by acceptor photobleaching to be 25% and 37%, respectively, before and after FsK stimulation. These numbers are somewhat higher than the *in vitro* estimates from Fig. 2*A*. Mutations S475A and K280E, which, respectively, abolished and greatly reduced the FRET responses *in vitro*, had the same effects in intact HeLa cells (Fig. 3 *B* and *C*). The PKA-specific inhibitor, H-89 (34), also blocked the response of the unmutated reporter (Fig. 3*C*). Despite the *in vitro* reversibility of the reporter, removal of cAMP and addition of H-89 did not reverse the FRET response in cells (data not shown). This may be because protein phosphatase-1 is largely nuclear (35, 36) whereas the reporter is cytosolic. It also could reflect the generation of the activated form of protein phosphatase inhibitor 1, which would keep protein phosphatase-1 in its inactive state (37).

To compare the FRET change with the phosphorylation state of the reporter, immunoblotting analysis was performed by using antiphospho-PKA-substrate antibody before and after stimulation with 50 μM FsK for 30 min. AKAR1 was of the expected molecular weight, showing no proteolysis, and FsK increased phosphorylation in correlation with the FRET increase (Fig. 3*A Right*). HEK293 cells and COS-7 cells transfected with AKAR1 gave FRET responses to cAMP elevations similar to those of HeLa cells. Chinese hamster ovary cells gave much higher starting emission ratios and smaller subsequent responses to FsK (≈5% increase), possibly indicating higher basal levels of PKA activity (data not shown).

Different means of elevating intracellular cAMP gave surprisingly different kinetics for the FRET increase (Fig. 3*D*). Bt_2cAMP is traditionally used as a membrane-permeant derivative of cAMP. However, even a very high dose of Bt_2cAMP (1 mM) required 10–15 min to produce a half-maximal increase in FRET, compared with 3–5 min for FsK stimulation. This result confirms that Bt_2cAMP is actually quite slow at crossing the plasma membrane and hydrolyzing to the active monobutyryl species (38). A more physiological stimulus, activation of β-adrenergic receptors with a selective agonist such as isoproterenol (100 μM), caused increases in FRET in 2–10 min, often with a variable lag time and a surprisingly sigmoidal time course. Many cells did not respond to isoproterenol at all, probably reflecting low and heterogeneous expression levels of endogenous β-adrenergic receptors in HeLa cells (39).

The fastest intracellular responses were generated by photolytic release ("uncaging") of cAMP from a membrane-permeant ester, DMNB-cAMP (40). When reporter-expressing cells preincubated with 50–200 μM DMNB-cAMP were exposed to UV for 5 sec to uncage the cAMP intracellularly, the emission ratio acutely increased by 15–25% in just 15–25 s, revealing much faster kinetics of the PKA response (Fig. 3*D*). The slower time courses of the other responses are presumably caused by rate-limiting steps in activating adenylate cyclase and accumulating sufficient cAMP, rather than the kinetics of activation of PKA by cAMP, the subsequent phosphorylation of the reporter, or the FRET response of the latter.

Kinetics of Tethered Constructs. A major example of potential regulation of an important kinase by submicroscopic localization is the anchoring of the regulatory (R) subunit of PKA to AKAPs (1–3). AKAPs are believed to play essential roles in controlling the specificity, magnitude, and duration of cAMP signaling and crosstalk with other pathways. AKAPs also can achieve integrated signaling by binding several signaling molecules together at the same site. Short peptides derived from the kinase binding domains of AKAPs can disrupt RII/AKAP interactions *in vitro* and inhibit certain cAMP-responsive events *in vivo* (41, 42). However, activation of PKA is classically considered to require release or unleashing of the diffusible catalytic (C) from the R subunit (43), so it remains unclear how much enhancement of phosphorylation results purely from pretethering a substrate near R.

To test the consequences of targeting PKA in close proximity to its substrate, we prepared several fusions of our AKAR1 to targeting and anchoring domains and directly monitored their phosphorylation inside cells (Fig. 4*A*). When fused to a nuclear localization signal, AKAR1 was appropriately targeted to the nucleus, where its response to FsK stimulation was somewhat smaller (15% emission ratio increase) and much slower (5–20 min) than the 1- to 5-min time course for cytoplasmically distributed untagged AKAR1 (Fig. 4*C*; see Movie 1, which is published as supporting information on the PNAS web site, www.pnas.org). The slow response in the nucleus is consistent with dissociation of C and R subunits in the cytoplasm upon cAMP elevation and slow diffusional translocation of the former into the nucleus (44, 45). By contrast, fusion of AKAR to the RIIα subunit decreased the response time to 0.5–1 min, consistent with an increase in local C subunit activity caused by tethering of R subunit to the reporter (Fig. 4*C*). Enhancement of phosphorylation caused by tethering still strictly depended on cAMP, because direct fusion of the PKA sensor to a dominant-negative mutant of RIIα (R213K) with a much weakened cAMP affinity (46, 47) gave a slower response than the untethered reporter (Fig. 4*C*). Pretethering the reporter to PKA holoenzyme also was effective even when noncovalent. Specifically, a short peptide RPP8, the PKA-binding domain of the anchoring protein D-AKAP2 (48), provided a mechanism of noncovalent tethering of endogenous PKA holoenzyme. Fusion of RPP8 to AKAR1 shortened the response time to FsK to 0.5–1.5 min (Fig. 4*C*), indistinguishable from that of the RIIα-AKAR1 fusion and notably faster than the untethered reporter, consistent with accelerated phosphorylation caused by local enrichment of C by noncovalent tethering of AKAR to PKA holoenzyme by means of the fused RPP8. Except for the nuclear-localized reporter, all of the fusions showed cytoplasmic distributions similar to the untethered reporter (Figs. 3*A* vs. 4*B*); thus the kinetic effects reflect localizations below the resolution of conventional fluorescence microscopy.

To resolve the kinetic effects of tethering more finely, we repeated the comparison of different reporter fusions in response to our fastest available mode of activation, photolytic uncaging of cAMP (Fig. 4*D*). Under these conditions, the fusion of AKAR1 with wild-type RIIα responded slightly faster than the reporter fused to RPP8, which in turn was faster than the unfused reporter. The reporter fused to mutant RIIα did not respond to uncaging 50 μM DMNB-cAMP (data not shown), but did respond to uncaging of 200 μM of DMNB-cAMP applied, albeit more slowly than all of the other reporter versions at this higher dose of caged compound. Presumably the uncaging of 200 but not 50 μM DMNB-cAMP elevated cAMP enough to activate the mutant holoenzyme. These results confirm the FsK experiments and provide a quantitative demonstration that deliberate submicroscopic redistribution of a substrate can modulate its susceptibility to phosphorylation by PKA.

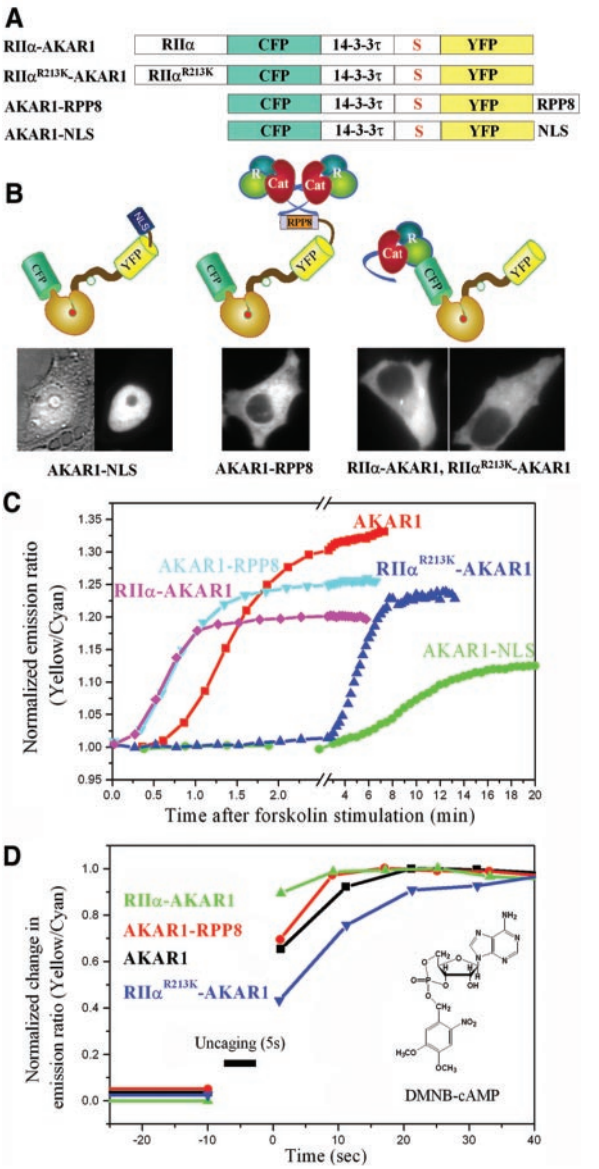

Fig. 4. Fusions of AKAR1 to targeting and recruitment domains. (*A*) Domain structures of the fusion constructs. (*B*) Schematic representation and cellular distribution of different fusions. The matched phase-contrast image on the left shows nuclear localization of the reporter. The height of the frames in *B* corresponds to 49 μm. (*C*) Emission ratio time courses for the untagged, RPP8-fused, wild-type RIIα-fused, mutant RIIα-fused and nuclear localization signal-tagged AKAR1 stimulated with FsK (50 μM). (*D*) Emission ratio time courses for the untagged, RPP8-fused, wild-type RIIα-fused, mutant RIIα-fused in response to uncaging of 200 μM of DMNB-cAMP.

Discussion

Signaling through cAMP and PKA remains one of the most important and exciting areas in cell biology and physiology. The present reporters of PKA activation have some unique advantages over previous methods for assessing activation of the cAMP signaling pathway inside cells. The most common method for measuring cAMP is RIA, but this technique requires destroying large amounts of cells or tissue, has very poor spatial and temporal resolution, and measures total rather than free cAMP. Measurements of the "activity ratio," i.e., activation state of endogenous PKA, are technically quite demanding and likewise destructive. Free cAMP can be imaged in single cells microinjected with fluorescein-labeled C subunits and rhodamine-labeled R subunits, which dissociate from each other and lose FRET upon elevation of cAMP. However, preparation and microinjection of the doubly labeled holoenzyme is not trivial. The amount of holoenzyme

introduced must considerably exceed the levels of endogenous PKA for FRET to recover after cAMP levels fall. This required excess may raise concerns about buffering of cAMP or perturbation of endogenous PKA localization (49, 50). The microinjection problem has been overcome by fusing two colors of GFP mutants to the C and R subunits such that FRET is disrupted by cAMP elevation (19), but the expression levels of the two fusions have to be approximately matched and still need to exceed endogenous PKA by a considerable margin. FRET between labeled R and C subunits measures the physical association of exogenous subunits, whereas the current indicator and that of Nagai *et al.* (26) are unitary constructs that report the catalytic activity of endogenous kinase. Because each kinase molecule should be able to phosphorylate a large number of substrate and reporter molecules, introduction of exogenous substrates should cause less buffering or perturbation than an equal number of exogenous kinase molecules, although this speculation remains to be proven experimentally. The emission ratio changes of the current phosphorylation reporter are also comparable to or larger than those of the fluorescent protein-labeled kinase subunits. Perhaps the greatest uncertainty with the present phosphorylation reporter is the extent to which it can be dephosphorylated in live cells, but this aspect should be improvable by further engineering if necessary.

Pretethering of the reporter to PKA holoenzyme accelerated the phosphorylation. Therefore, before the C subunit diffuses away to phosphorylate randomly located substrates in the cytoplasm or nucleus, it preferentially phosphorylates substrates tethered to the R subunit, which had previously been keeping C inactive. This example shows that deliberate redistribution of a substrate can modulate its susceptibility to phosphorylation by PKA. The rich variety of R subunit-anchoring proteins and the ability of active C subunit to dissociate from R means that PKA signaling is a particularly interesting system for studying the effects of kinase and substrate localization. As PKA is typically part of a large molecular assembly, we are now poised to ask questions about signal integration by bringing in phosphatases (51) and phosphodiesterases (52). The genetically encoded reporter also can be targeted to various subcellular locations, such as plasma membrane, mitochondria, endoplasmic reticulum, and Golgi to investigate cAMP signaling events in each location. The successful design of AKAR and its application for studying compartmentalized and dynamic modulation of kinases has laid a foundation for studying targeting and compartmentation of PKA and other kinases and phosphatases.

We thank S. R. Adams, R. E. Campbell, L. A. Gross, T. Hunter, M. C. Mumby, A. Newton, R. B. Pilz, P. Steinbach, A. S. Shaw, and A. Y. Ting for assistance and advice. This work was supported by the National Institutes of Health (Grant NS27177 to R.Y.T. and Grant DK54441 to S.S.T.), Howard Hughes Medical Institute (R.Y.T. and S.S.T.), and Alliance for Cellular Signaling Grant GM62114 (J.Z. and R.Y.T.).

1. Skalhegg, B. S. & Tasken, K. (2000) *Front. Biosci.* **5,** D678–D693.
2. Edwards, A. S. & Scott, J. D. (2000) *Curr. Opin. Cell Biol.* **12,** 217–221.
3. Feliciello, A., Gottesman, M. E. & Avvedimento, E. V. (2001) *J. Mol. Biol.* **308,** 99–114.
4. Vijayaraghavan, S., Liberty, G. A., Mohan, J., Winfrey, V. P., Olson, G. E. & Carr, D. W. (1999) *Mol. Endocrinol.* **13,** 705–717.
5. Klussmann, E., Maric, K., Wiesner, B., Beyermann, M. & Rosenthal, W. (1999) *J. Biol. Chem.* **274,** 4934–4938.
6. Mochly-Rosen, D. (1995) *Science* **268,** 247–251.
7. Frame, S., Cohen, P. & Biondi, R. M. (2001) *Mol. Cell* **7,** 1321–1327.
8. Czernik, A. J., Girault, J.-A., Nairn, A. C., Chen, J., Snyder, G., Kebabian, J. & Greengard, P. (1991) *Methods Enzymol.* **201,** 264–283.
9. Verveer, P. J., Wouters, F. S., Reynolds, A. R. & Bastiaens, P. I. (2000) *Science* **290,** 1567–1570.
10. Ng, T., Squire, A., Hansra, G., Bornancin, F., Prevostel, C., Hanby, A., Harris, W., Barnes, D., Schmidt, S., Mellor, H., *et al.* (1999) *Science* **283,** 2085–2089.
11. Post, P. L., Trybus, K. M. & Taylor, D. L. (1994) *J. Biol. Chem.* **269,** 12880–12887.
12. Higashi, H., Sato, K., Omori, A., Sekiguchi, M., Ohtake, A. & Kudo, Y. (1996) *NeuroReport* **7,** 2695–2700.
13. Higashi, H., Sato, K., Ohtake, A., Omori, A., Yoshida, S. & Kudo, Y. (1997) *FEBS Lett.* **414,** 55–60.
14. Lee, C. L., Linton, J., Soughayer, J. S., Sims, C. E. & Allbritton, N. L. (1999) *Nat. Biotechnol.* **17,** 759–762.
15. Romoser, V. A., Hinkle, P. M. & Persechini, A. (1997) *J. Biol. Chem.* **272,** 13270–13274.
16. Miyawaki, A., Llopis, J., Heim, R., McCaffery, J. M., Adams, J. A., Ikura, M. & Tsien, R. Y. (1997) *Nature (London)* **388,** 882–887.
17. Griesbeck, O., Baird, G. S., Campbell, R. E., Zacharias, D. A. & Tsien, R. Y. (2001) *J. Biol. Chem.* **276,** 29188–29194.
18. Miyawaki, A. & Tsien, R. Y. (2000) *Methods Enzymol.* **327,** 472–500.
19. Zaccolo, M., De Giorgi, F., Cho, C. Y., Feng, L., Knapp, T., Negulescu, P. A., Taylor, S. S., Tsien, R. Y. & Pozzan, T. (2000) *Nat. Cell Biol.* **2,** 25–29.
20. Sato, M., Hida, N., Ozawa, T. & Umezawa, Y. (2000) *Anal. Chem.* **72,** 5918–5924.
21. Honda, A., Adams, S. R., Sawyer, C. L., Lev-Ram, V., Tsien, R. Y. & Dostmann, W. R. G. (2001) *Proc. Natl. Acad. Sci. USA* **98,** 2437–2442.
22. Heim, R. & Tsien, R. Y. (1996) *Curr. Biol.* **6,** 178–182.
23. Mitra, R. D., Silva, C. M. & Youvan, D. C. (1996) *Gene* **173,** 13–17.
24. Mahajan, N. P., Harrison-Shostak, D. C., Michaux, J. & Herman, B. (1999) *Chem. Biol.* **6,** 401–409.
25. Mochizuki, N., Yamashita, S., Kurokawa, K., Ohba, Y., Nagai, T., Miyawaki, A. & Matsuda, M. (2001) *Nature (London)* **411,** 1065–1068.
26. Nagai, Y., Miyazaki, M., Aoki, R., Zama, T., Inouye, S., Hirose, K., Iino, M. & Hagiwara, M. (2000) *Nat. Biotechnol.* **18,** 313–316.
27. Muslin, A. J., Tanner, J. W., Allen, P. M. & Shaw, A. S. (1996) *Cell* **84,** 889–897.
28. Huang, P. L., Dawson, T. M., Bredt, D. S., Snyder, S. H. & Fishman, M. C. (1993) *Cell* **75,** 1273–1286.
29. Fu, H., Subramanian, R. R. & Masters, S. C. (2000) *Annu. Rev. Pharmacol. Toxicol.* **40,** 617–647.
30. Aitken, A., Jones, D., Soneji, Y. & Howell, S. (1995) *Biochem. Soc. Trans.* **23,** 605–611.
31. Yaffe, M. B., Rittinger, K., Volinia, S., Caron, P. R., Aitken, A., Leffers, H., Gamblin, S. J., Smerdon, S. J. & Cantley, L. C. (1997) *Cell* **91,** 961–971.
32. Kemp, B. E. (1980) *J. Biol. Chem.* **255,** 2914–2918.
33. Zhang, L., Wang, H., Liu, D., Liddington, R. & Fu, H. (1997) *J. Biol. Chem.* **272,** 13717–13724.
34. Chijiwa, T., Mishima, A., Hagiwara, M., Sano, M., Hayashi, K., Inoue, T., Naito, K., Toshioka, T. & Hidaka, H. (1990) *J. Biol. Chem.* **265,** 5267–5272.
35. Haneji, T., Morimoto, H., Morimoto, Y., Shirakawa, S., Kobayashi, S., Kaneda, C., Shima, H. & Nagao, M. (1998) *Biochem. Biophys. Res. Commun.* **248,** 39–43.
36. Allen, P. B., Kwon, Y. G., Nairn, A. C. & Greengard, P. (1998) *J. Biol. Chem.* **273,** 4089–4095.
37. Oliver, C. J. & Shenolikar, S. (1998) *Front. Biosci.* **3,** D961–D972.
38. Schultz, C., Vajanaphanich, M., Genieser, H. G., Jastorff, B., Barrett, K. E. & Tsien, R. Y. (1994) *Mol. Pharmacol.* **46,** 702–708.
39. Duman, R. S., Fishman, P. H. & Tallman, J. F. (1994) *J. Recept. Res.* **14,** 1–10.
40. Nerbonne, J. M., Richard, S., Nargeot, J. & Lester, H. A. (1984) *Nature (London)* **310,** 74–76.
41. Scott, J. D. & Faux, M. C. (1998) *Methods Mol. Biol.* **88,** 161–185.
42. Carr, D. W., Hausken, Z. E., Fraser, I. D., Stofko-Hahn, R. E. & Scott, J. D. (1992) *J. Biol. Chem.* **267,** 13376–13382.
43. Taylor, S. S., Buechler, J. A. & Yonemoto, W. (1990) *Annu. Rev. Biochem.* **59,** 971–1005.
44. Meinkoth, J. L., Ji, Y., Taylor, S. S. & Feramisco, J. R. (1990) *Proc. Natl. Acad. Sci. USA* **87,** 9595–9599.
45. Harootunian, A. T., Adams, S. R., Wen, W., Meinkoth, J. L., Taylor, S. S. & Tsien, R. Y. (1993) *Mol. Biol. Cell* **4,** 993–1002.
46. Hemmer, W., McGlone, M. & Taylor, S. S. (1997) *Anal. Biochem.* **245,** 115–122.
47. Houslay, M. D. & Milligan, G. (1997) *Trends Biochem. Sci.* **22,** 217–224.
48. Huang, L. J., Durick, K., Weiner, J. A., Chun, J. & Taylor, S. S. (1997) *Proc. Natl. Acad. Sci. USA* **94,** 11184–11189.
49. Adams, S. R., Harootunian, A. T., Buechler, Y. J., Taylor, S. S. & Tsien, R. Y. (1991) *Nature (London)* **349,** 694–697.
50. Adams, S. R., Bacskai, B. J., Taylor, S. S. & Tsien, R. Y. (1993) in *Fluorescent Probes for Biological Activity of Living Cells: A Practical Guide*, ed. Mason, W. T. (Academic, New York), pp. 133–149.
51. Schillace, R. V., Voltz, J. W., Sim, A. T., Shenolikar, S. & Scott, J. D. (2001) *J. Biol. Chem.* **276,** 12128–12134.
52. Dodge, K. L., Khouangsathiene, S., Kapiloff, M. S., Mouton, R., Hill, E. V., Houslay, M. D., Langeberg, L. K. & Scott, J. D. (2001) *EMBO J.* **20,** 1921–1930.